Particle energy study with Particle in Cell methods

Non ideal Magnetohydrodynamics

- Particle species treated as a fluid.
- Low-frequency, large scale magnetic behavior.
- Continuity equation, equation of motion, equation of state, Ampère's law, Faraday's law, and Ohm's law.

In ideal MHD no magnetic energy can convert to kinetic energy.
Non-ideal MHD: resistivity $\rightarrow$ instabilities, particle acceleration, emmision.

Magnetic Reconnection

Oppositely directed magnetic field lines, current density in between with width δ.

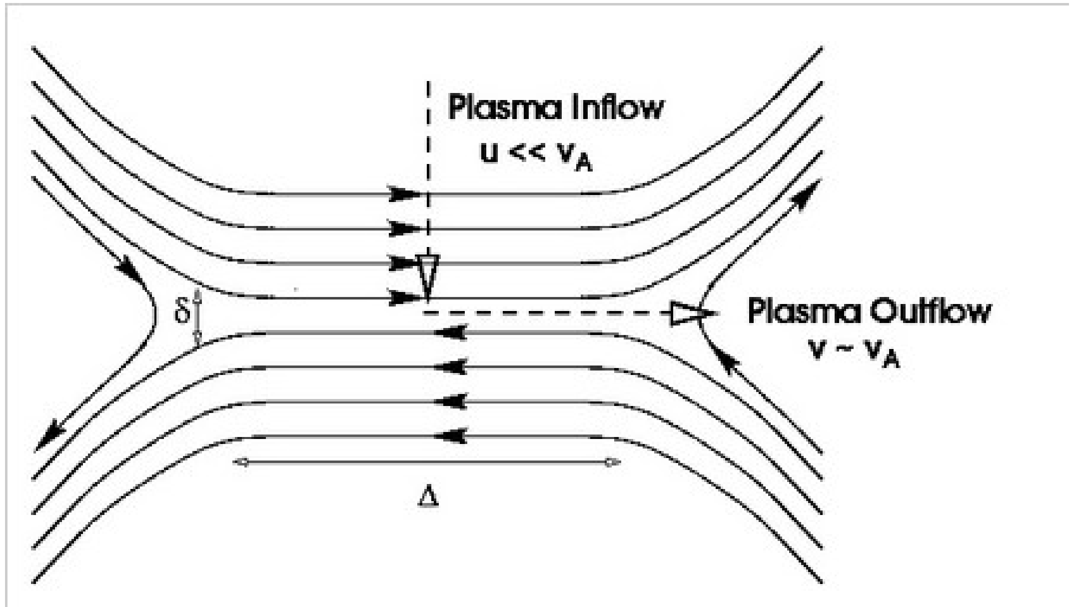

Force Free magnetic fields

A magnetic field in which the Lorentz force is equal to zero and the magnetic pressure greatly exceeds the plasma pressure such that non-magnetic forces can be neglected.

Pulsar magnetospheres, AGN jets, stellar surface.

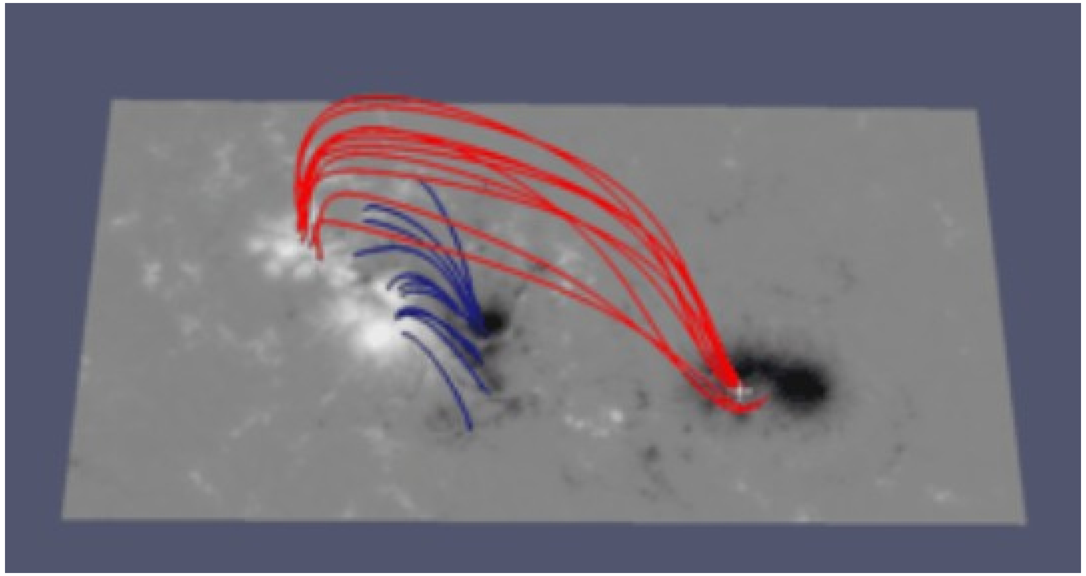

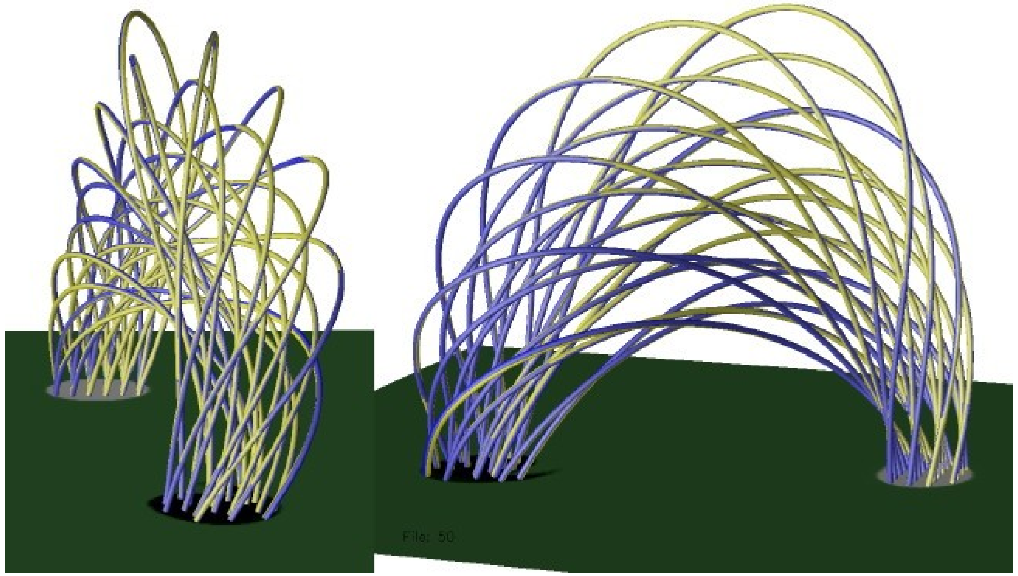

Vlasov equation

Two numerical approaches to solve Vlasov

$$\boxed{\frac{\partial f}{\partial t}+\frac{\boldsymbol{p}}{\gamma m}\cdot\frac{\partial f}{\partial \boldsymbol{r}}+q\left(\boldsymbol{E}+\frac{\boldsymbol{v}\times\boldsymbol{B}}{c}\right)\cdot\frac{\partial f}{\partial \boldsymbol{p}}=0}$$

Ab-initio model, no approximations

Directly with a Vlasov-code

Treat phase space as a continuum fluid

Advantages:

- **No noise**, good if tail of f is important dynamically (steep power-law).
- No issue if plasma very **inhomogeneous**.
- **Weak** phenomena can be captured

Limitations:

- Problem **(6+1)D**, hard to fit in the memory, limited resolution.
- Filamentation of the phase space

But becoming more competitive, new development to come, stay tuned!

Not covered here

Indirectltly with a PIC code

Sample phase space with particles

Advantages:

- Conceptually **simple**
- **Robust** and **easy to implement.**
- Easily **scalable** to large number of cores

Limitations:

- **Shot noise**, difficult to sample uniformly f,
- Artificial collisions, requires many particles
- Hard to capture weak/subtle phenomenas
- Load-balancing issues

10

Main focus of this lecture

B. Cerutti

Knowing the distribution function of the particles, and the forces acting on them, we can follow their evolution on phase space. Boltzmann equation does not work. (Coulomb interaction)

6 degrees of freedom (position, momentum).
We assume collisionless plasma.

An exact solution of the steady-state, one-dimensional Vlasov–Maxwell equations for a plasma current sheet with oppositely directed magnetic field was found by Harris in 1962. The so-called Harris magnetic field model assumes Maxwellian velocity distributions for oppositely drifting ions and electrons and has been widely used for plasma stability studies.

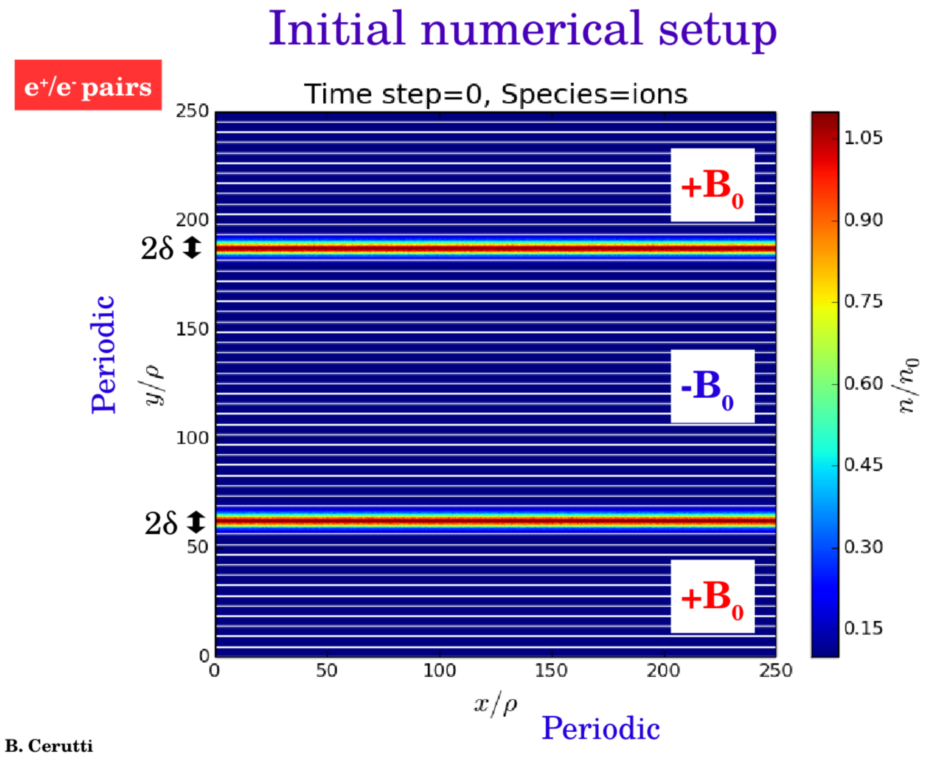

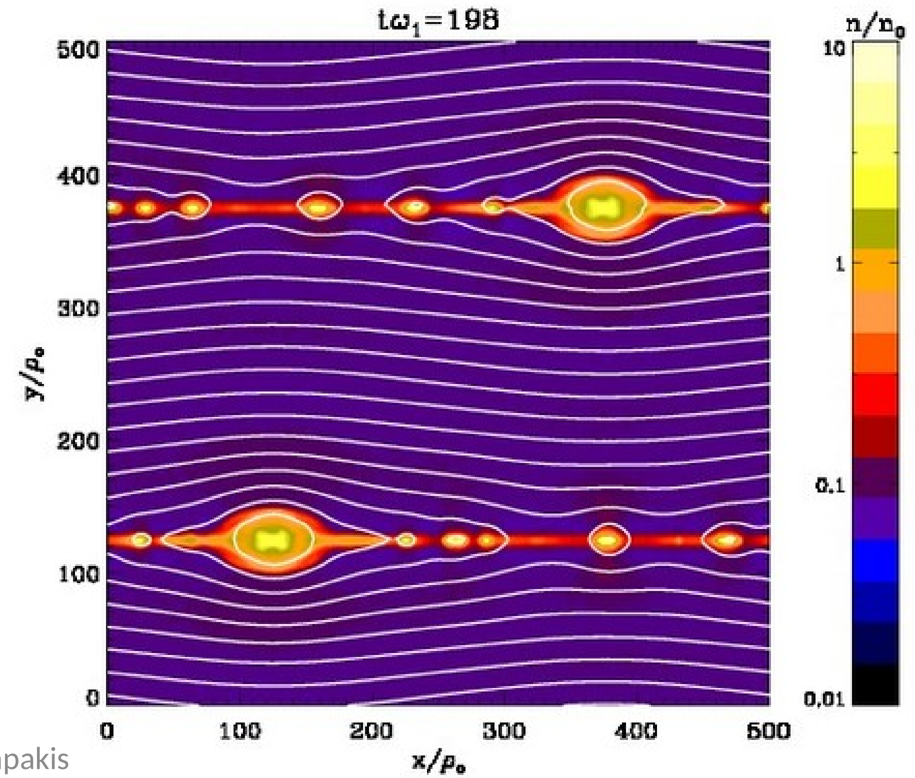

Gromeka-Arnold-Beltrami-Childress flow

Three-dimensional incompressible velocity field which is an exact solution of Euler's equation. In Cartesian coordinates:

Early numerical experiments by Henon (1966) have provided evidence for chaos in the special case A = √3, B = √2, C = 1. The special case A = B = C = 1 was introduced independently by Childress (1967, 1970) as a model for the kinematic dynamo effect. We propose to call these flows ABC (for Arnold, Beltrami, Childress).

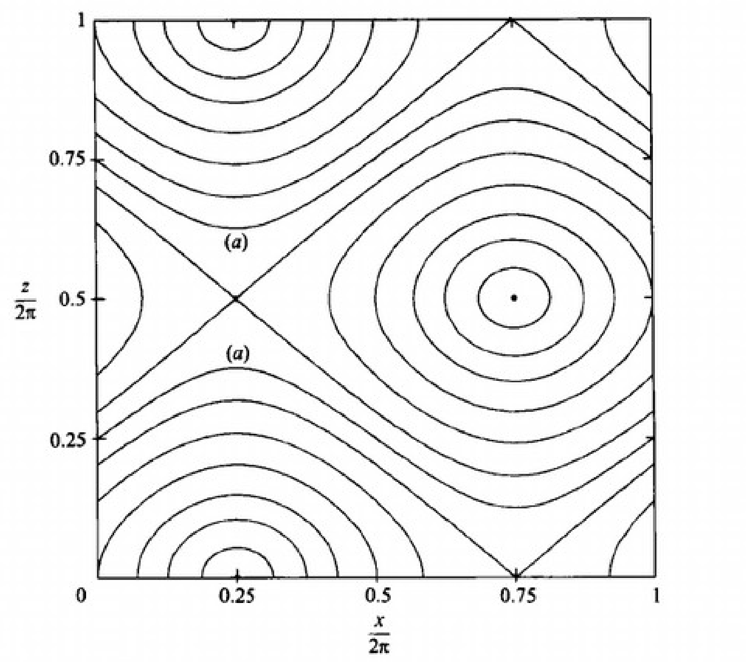

FIGURE 3. The integrable case: projection of streamlines on (x, z)-plane.

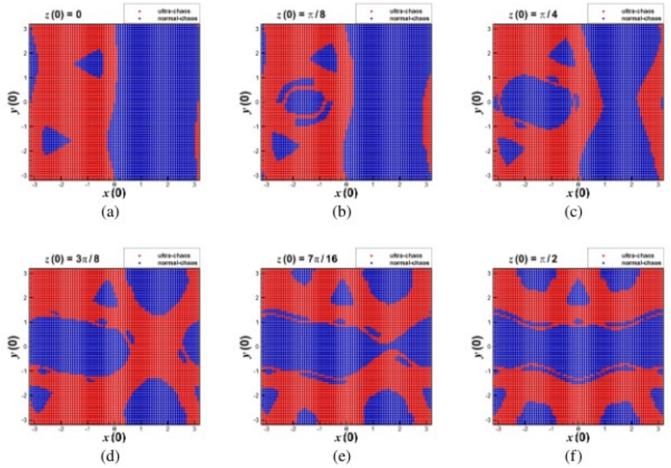

Zeltron Particle in Cell code

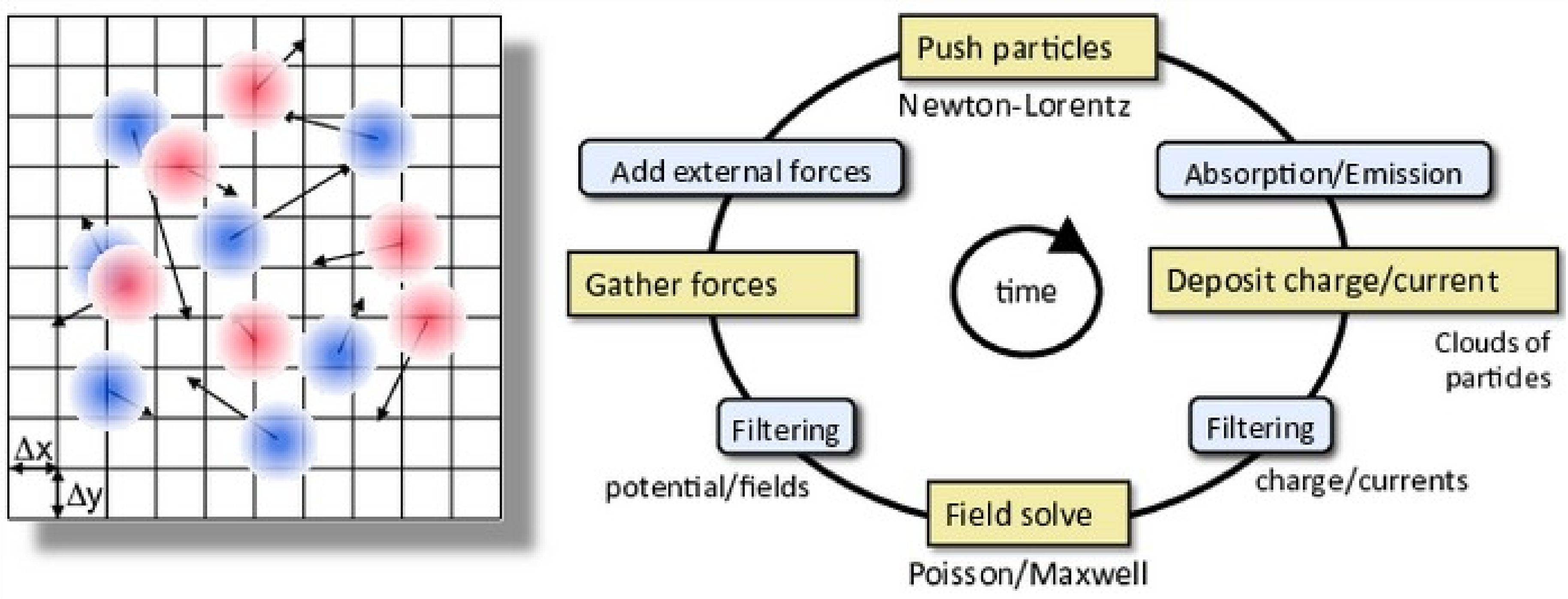

Particle interactions

Depending on the system, we might be interested in:

- electron-positron species,
- electron-proton species,
- proton-proton, dust particles with charged etc.

Hybrid PIC Monte Carlo collision algorithms provide a way to study these systems.

Limitations:

Known limitations with known consequence: Field discretization

- Spatial step $\Delta_x \approx$ Debye length $\lambda_d = v_t/\omega_p$.
- Numerical stability $\rightarrow$ small time step Δ_t.
  For my code: $\Delta_t = N_c\Delta_x/\sqrt{2}\,c$ with $0 < N_c < 1$.
- We have $\Delta_x = v_t/\omega_p$ and for $N_c = 1$ we get $\sqrt{2}\Delta_t\omega_p = v_t/c$.
  $\Rightarrow$ Low v_t requires high sampling rate. Critical speed $v_t \approx 10^6 m/s$.

Known limitations with unknown consequence:

Particle per cell count rates follow Poisson statistics $\rightarrow$ For N_e particles per cell, the relative fluctuations are $1/\sqrt{N_e}$.

- Fluctuations result in particle-wave collisions.
- Parametric instabilities speed up.
- Dispersive properties change. Bernstein modes are damped 'close' to $n\omega_c$.
- Signal-to-noise ratio is low.

Dieckmann, Frederiksen, Bret, Shukla, Phys. Plasmas 13, 113110 (2006).

Test cases: Two stream instability

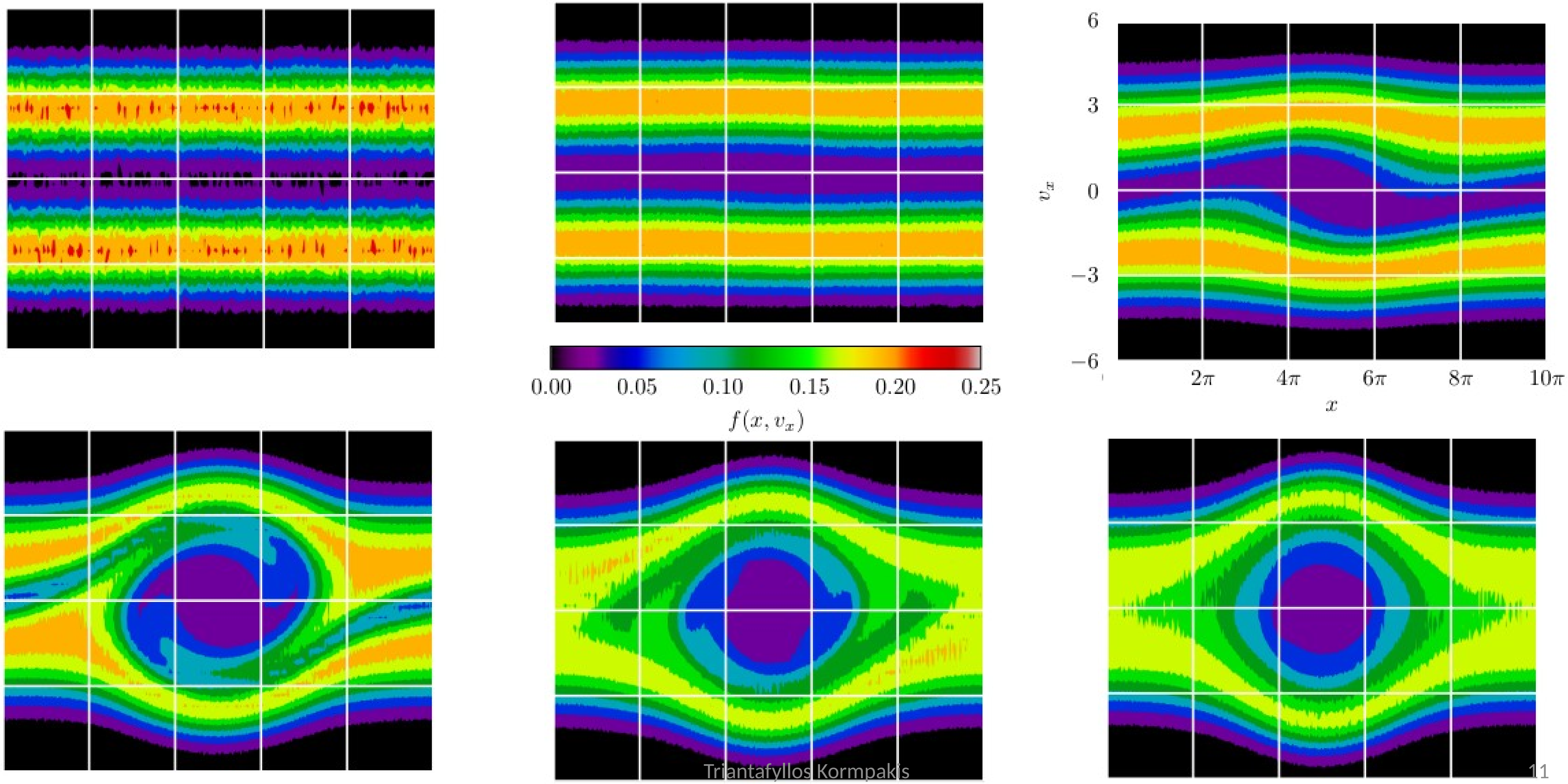

Yee finite difference time domain

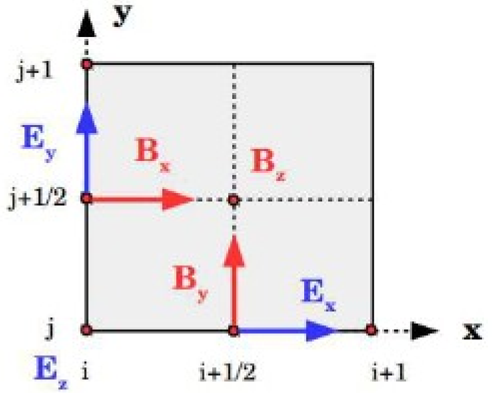

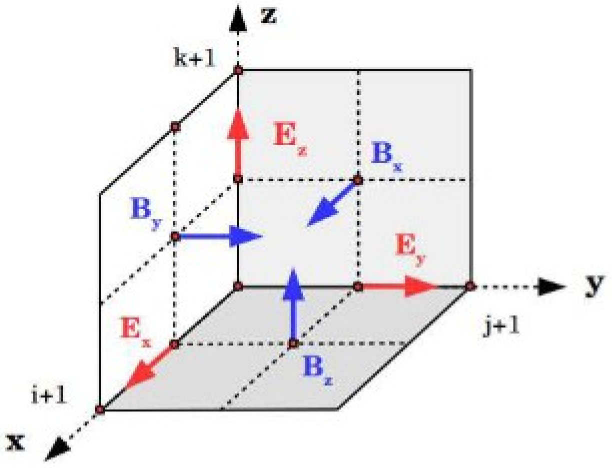

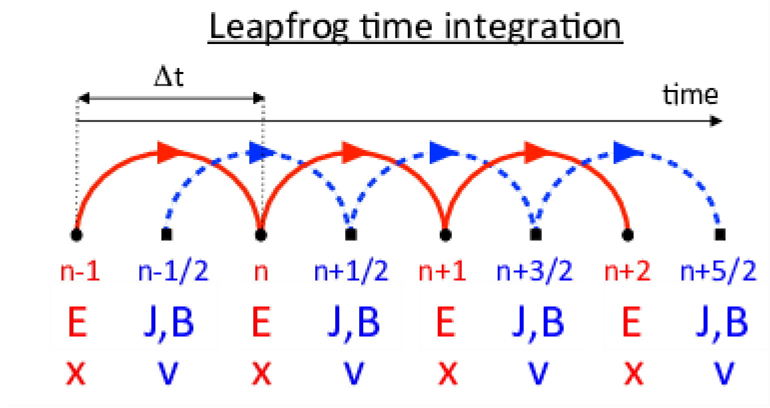

Boris particle push

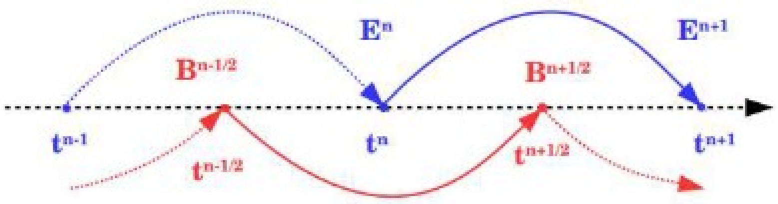

Particle weighting

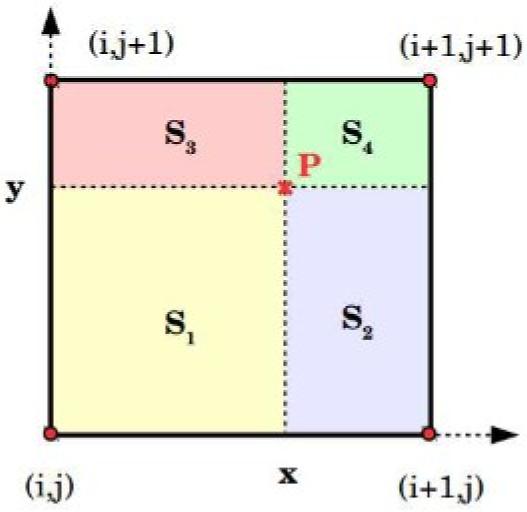

Very **robust** and **stable** if the **Courant-Friedrichs-Lewy** (CFL) condition is fulfilled:

1D: $\left(\frac{c\,\Delta t}{\Delta x}\right)^2 < 1$ **2D:** $(c\,\Delta t)^2\left(\frac{1}{\Delta x^2}+\frac{1}{\Delta y^2}\right) < 1$ **3D:** $(c\,\Delta t)^2\left(\frac{1}{\Delta x^2}+\frac{1}{\Delta y^2}+\frac{1}{\Delta z^2}\right) < 1$

Polar coordinates

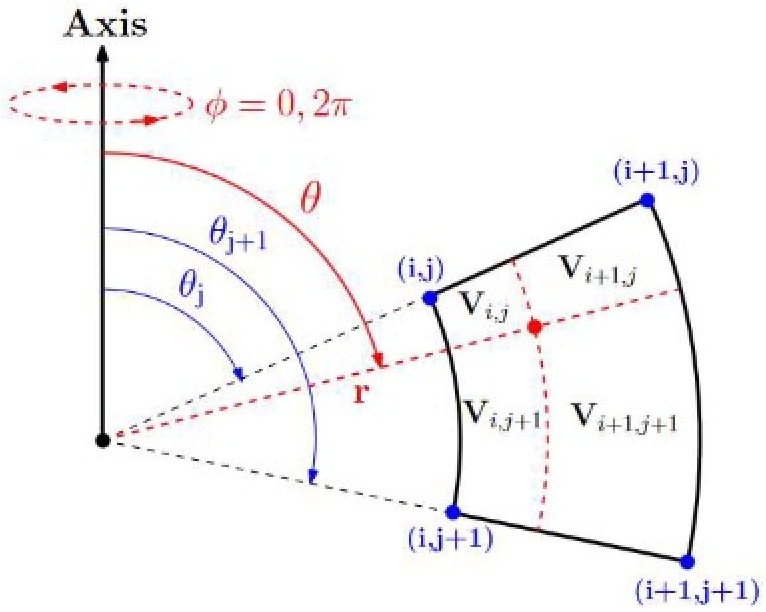

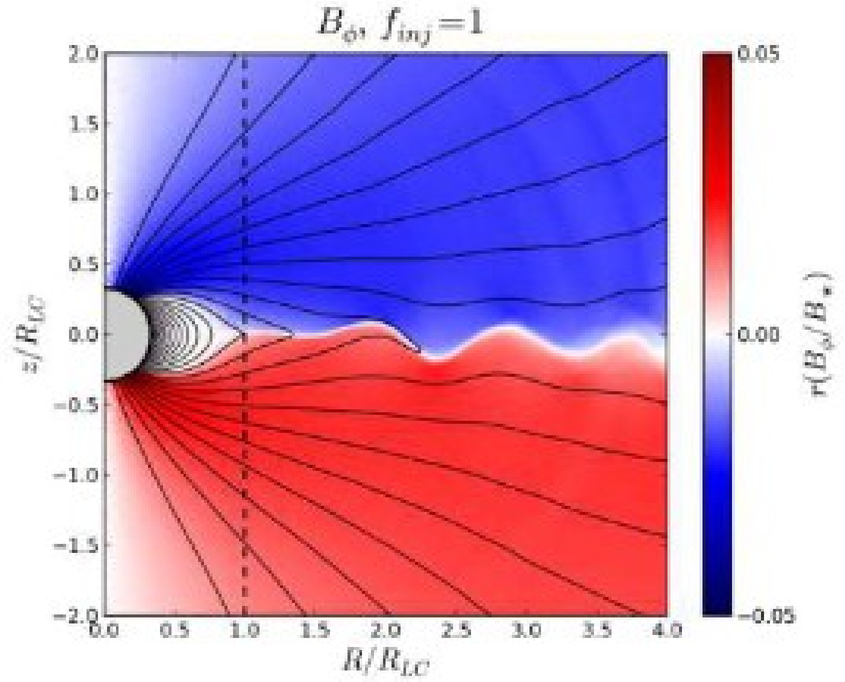

Cylindrical to cartesian coordinates

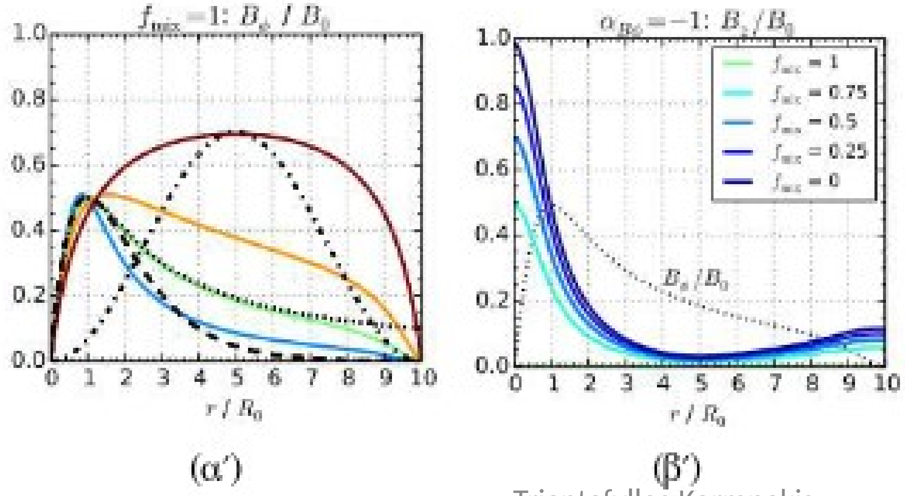

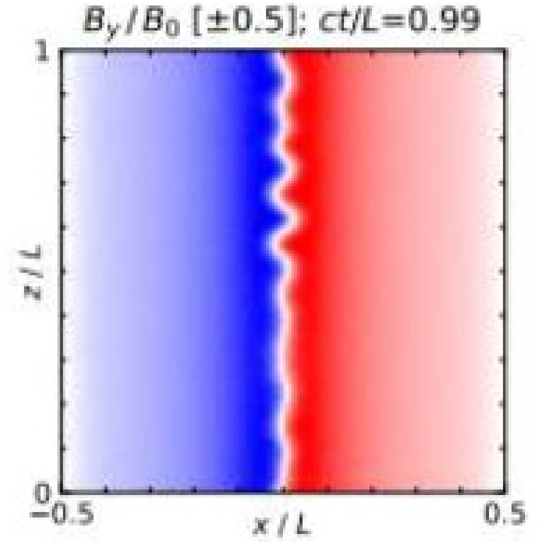

Insert Maxwellian distribution, Magnetic field configuration, current densities, define system wavenumber, grid size in each direction.

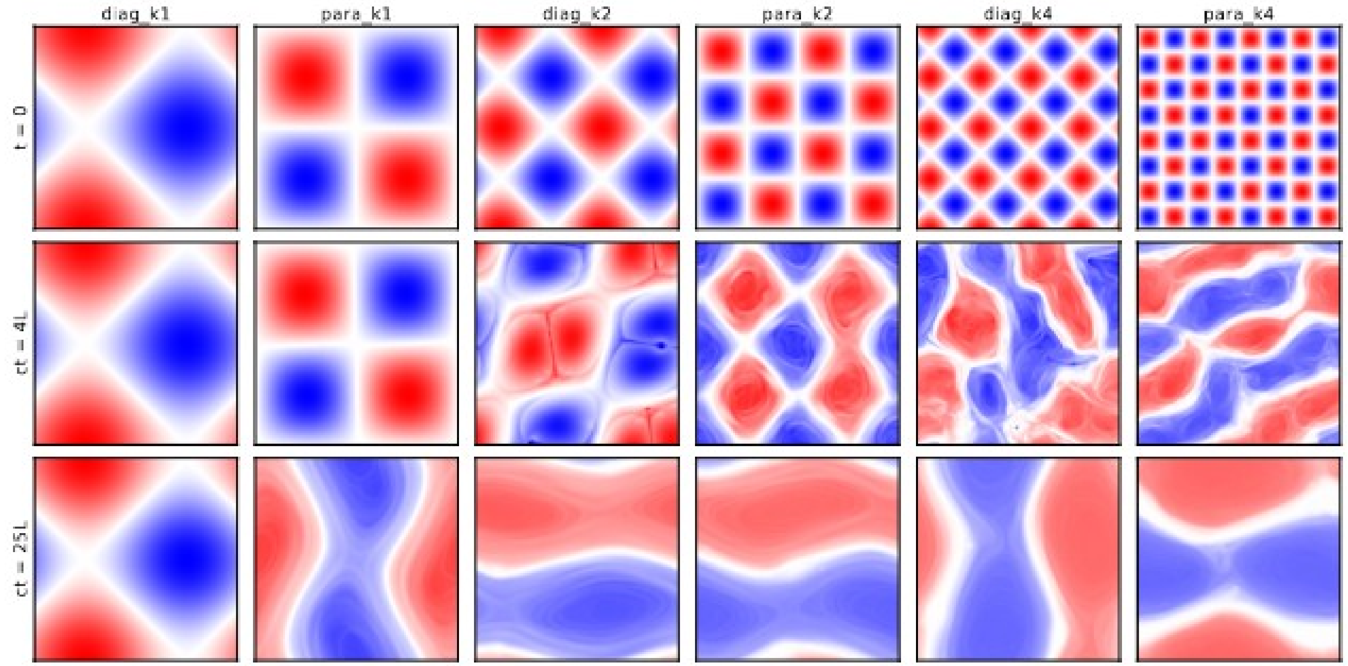

FIGURE 1. Spatial distributions of the out-of-plane magnetic field component B_z for ABC fields of different initial topologies. Each column of panels compares the initial configuration at $ct/L = 0$ (top) with an intermediate state at $ct/L \simeq 4$ (middle), and with the final state at $ct/L \simeq 25$ (bottom).

Chen et al. 2021

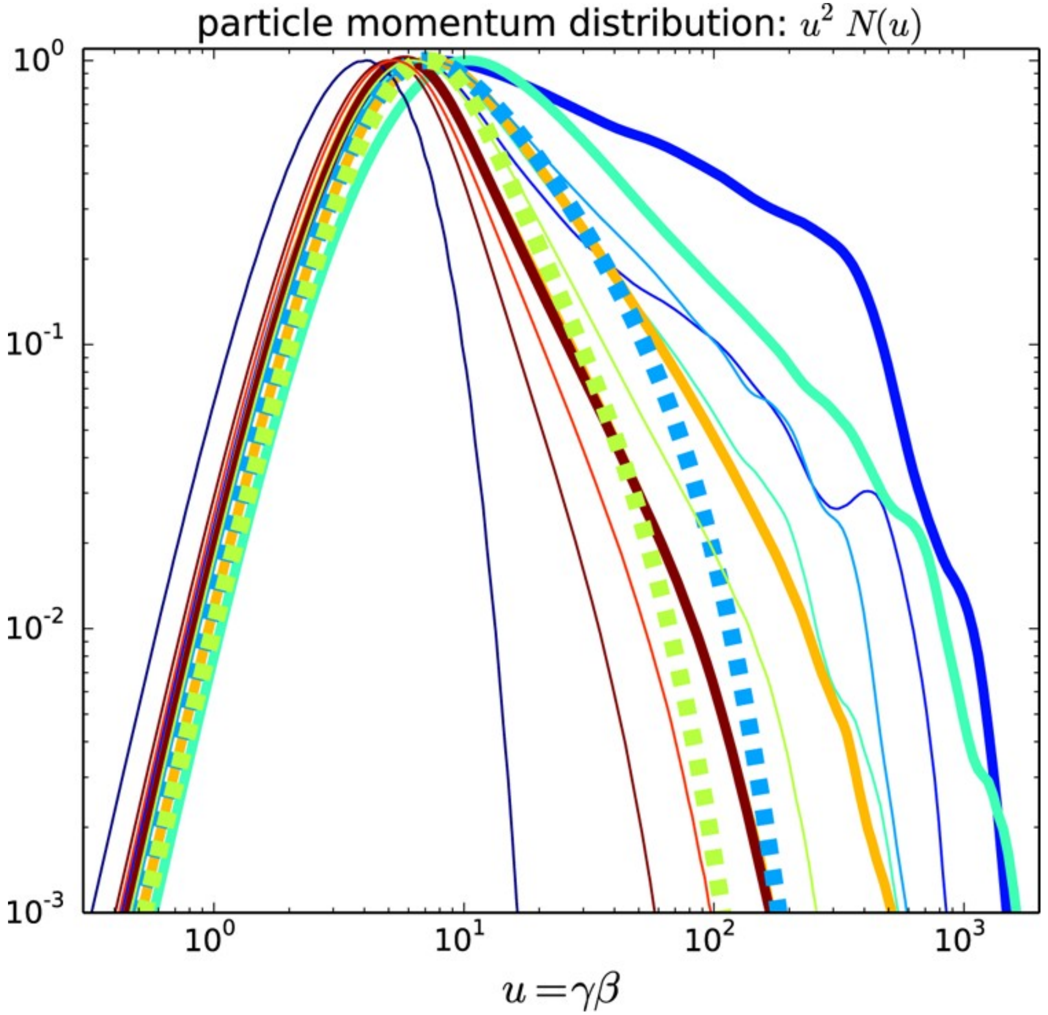

Config.	$\frac{L}{\lambda_0}$	$\tilde{a}_1$	$\frac{\rho_0}{\Delta x}$	$\langle \sigma_{\mathrm{ini}} \rangle$	$\mathcal{E}_{B,\mathrm{ini}}$	$\epsilon_{\mathrm{diss,fin}}$	$\tau_{E,\mathrm{peak}}$	p	$\gamma_{\max}$	f_E
2-D small, $N_x = 1728$										
para_k1	$\sqrt{2}$	1/4	2.4	2.8	0.65	0.26	0.25	3.1	450	0.18
para_k2	$2\sqrt{2}$	1/4	2.4	1.4	0.48	0.52	0.17	3.75	190	0.16
para_k4	$4\sqrt{2}$	1/4	2.4	0.7	0.31	0.59	0.14	4.8	60	0.07
para_k8	$8\sqrt{2}$	1/4	2.4	0.4	0.19	0.65	0.17	—	30	0.02
2-D medium, $N_x = 3456$										
para_k1	$\sqrt{2}$	1/4	2.4	5.6	0.78	0.27	0.21	2.85	870	0.31
diag_k2	2	1/4	2.4	4.0	0.72	0.44	0.16	2.95	620	0.34
para_k2	$2\sqrt{2}$	1/4	2.4	2.8	0.65	0.53	0.13	3.2	590	0.28
diag_k4	4	1/4	2.4	2.0	0.56	0.57	0.11	3.65	270	0.20
para_k4	$4\sqrt{2}$	1/4	2.4	1.4	0.48	0.59	0.09	3.8	190	0.15
diag_k8	8	1/4	2.4	1.0	0.39	0.60	0.08	4.2	100	0.10
para_k8	$8\sqrt{2}$	1/4	2.4	0.7	0.31	0.61	0.08	4.8	60	0.06
para_k1	$\sqrt{2}$	1/8	2.4	2.8	0.64	0.26	0.27	3.35	320	0.18
para_k1	$\sqrt{2}$	1/16	2.4	1.4	0.48	0.26	0.40	4.5	80	0.07
para_k1	$\sqrt{2}$	1/32	2.4	0.7	0.31	0.25	0.68	—	30	0.02
para_k2	$2\sqrt{2}$	1/8	2.4	1.4	0.48	0.51	0.19	4.2	150	0.13
para_k2	$2\sqrt{2}$	1/16	2.4	0.7	0.31	0.48	0.34	—	50	0.04
para_k4	$4\sqrt{2}$	1/8	2.4	0.7	0.31	0.57	0.17	5.2	60	0.05
para_k4	$4\sqrt{2}$	1/16	2.4	0.4	0.19	0.54	0.46	—	30	0.01
para_k8	$8\sqrt{2}$	1/8	2.4	0.4	0.19	0.58	0.20	—	30	0.01
para_k1	$\sqrt{2}$	1/4	4.8	2.8	0.64	0.26	0.25	3.2	410	0.18
para_k1	$\sqrt{2}$	1/4	9.6	1.4	0.48	0.26	0.32	3.8	160	0.10
para_k1	$\sqrt{2}$	1/4	19.2	0.7	0.31	0.27	0.44	5.8	40	0.05
para_k2	$2\sqrt{2}$	1/4	4.8	1.4	0.48	0.52	0.17	3.75	200	0.17
para_k2	$2\sqrt{2}$	1/4	9.6	0.7	0.31	0.52	0.30	—	50	0.10
para_k4	$4\sqrt{2}$	1/4	4.8	0.7	0.31	0.58	0.13	4.75	60	0.09
para_k4	$4\sqrt{2}$	1/4	9.6	0.4	0.19	0.63	0.24	—	30	0.05
para_k8	$8\sqrt{2}$	1/4	4.8	0.4	0.19	0.64	0.15	—	30	0.03
2-D large, $N_x = 6912$										
para_k1	$\sqrt{2}$	1/4	2.4	11.2	0.88	0.26	0.18	2.4	1490	0.56
para_k2	$2\sqrt{2}$	1/4	2.4	5.6	0.78	0.53	0.10	2.95	1620	0.40
para_k4	$4\sqrt{2}$	1/4	2.4	2.8	0.65	0.60	0.07	3.3	510	0.26
para_k8	$8\sqrt{2}$	1/4	2.4	1.4	0.48	0.61	0.05	3.85	170	0.12
3-D, $N_x = 1152$										
diag_k2	2	1/5	1.28	3.6	0.71	0.50	0.22	3.2	180	0.25
diag_k4	4	1/5	1.28	1.8	0.54	0.75	0.17	4.0	110	0.10

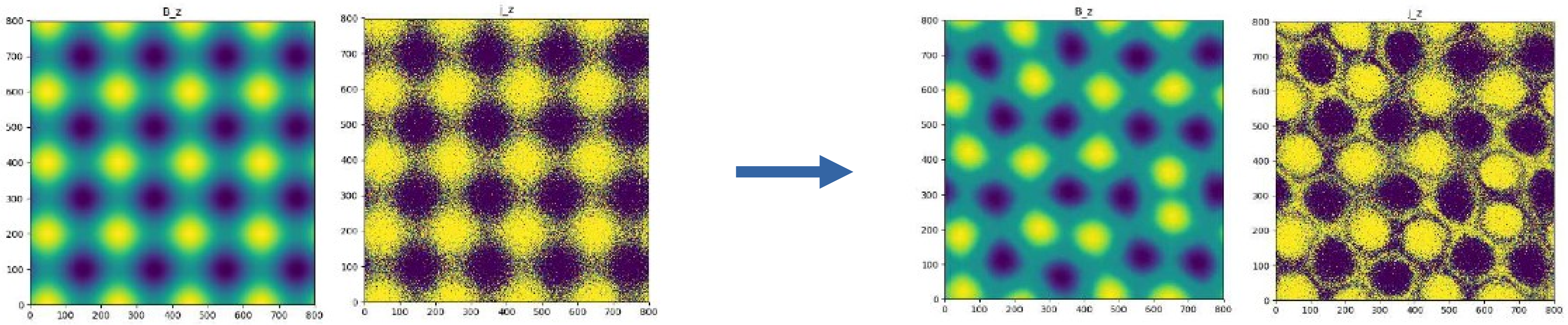

ABC magnetic field configurations. No current layers present. Periodical grid with coherence length
Grid resolution of simulations: 256 and 512.

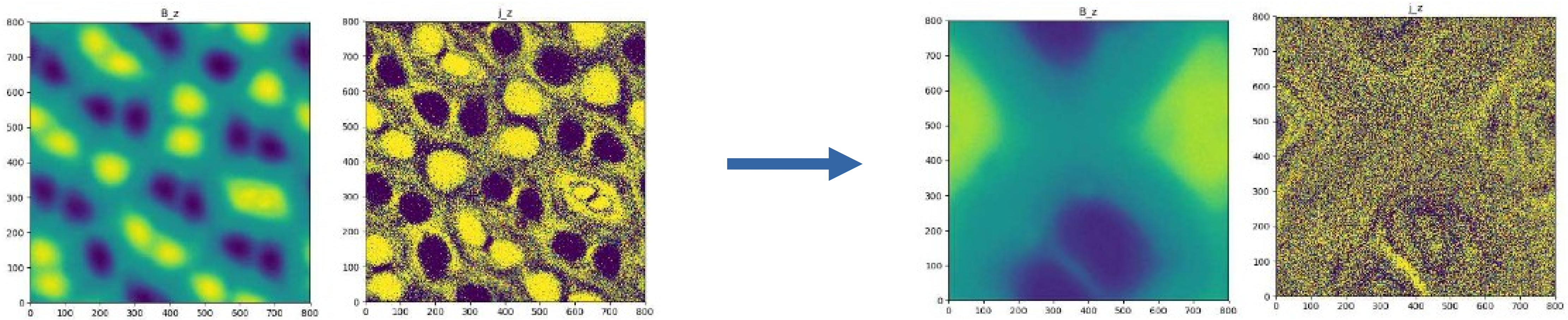

$$\Delta t = \frac{ct}{L} = \frac{0.99\Delta x\Delta y}{\sqrt{(\Delta x)^2+(\Delta y)^2}} = \frac{0.99\Delta x}{\sqrt{2}} = N_s\frac{0.99}{\sqrt{2}N_x}$$

Previous
system

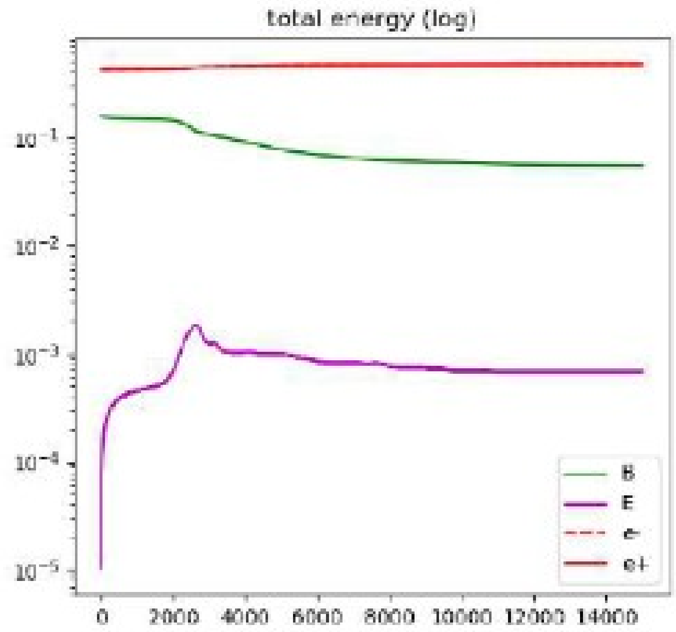

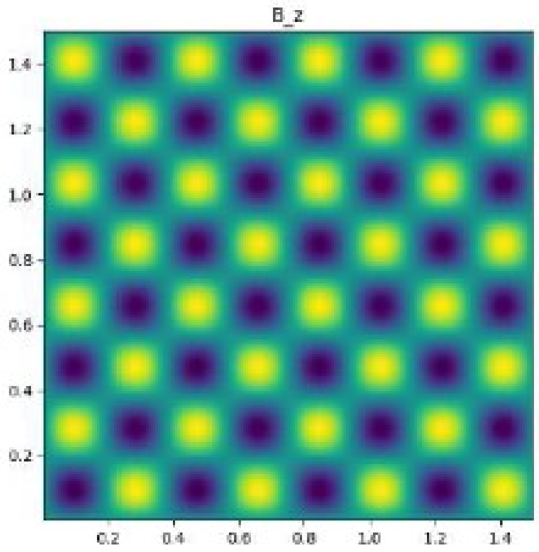

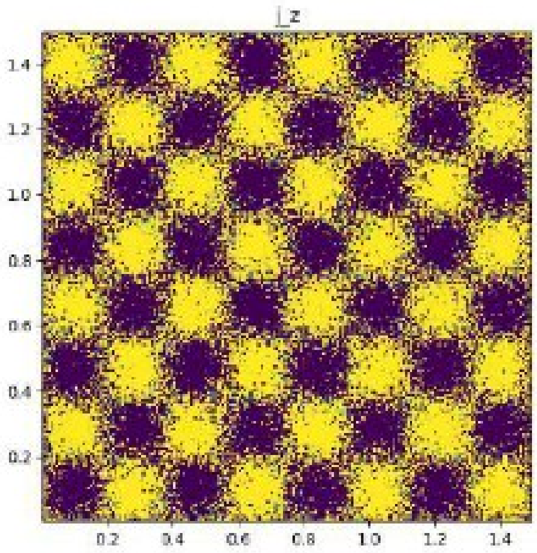

This
system

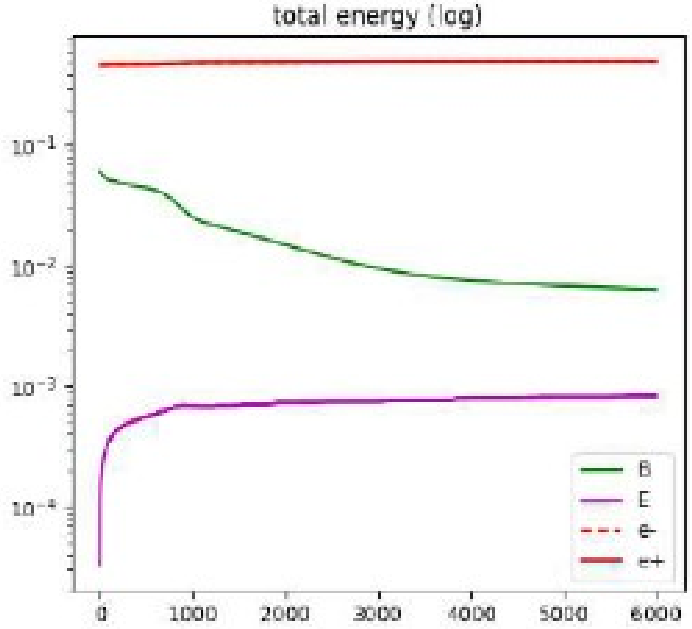

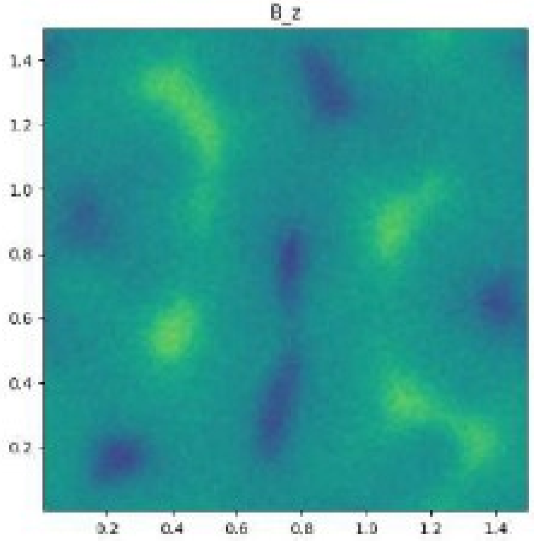

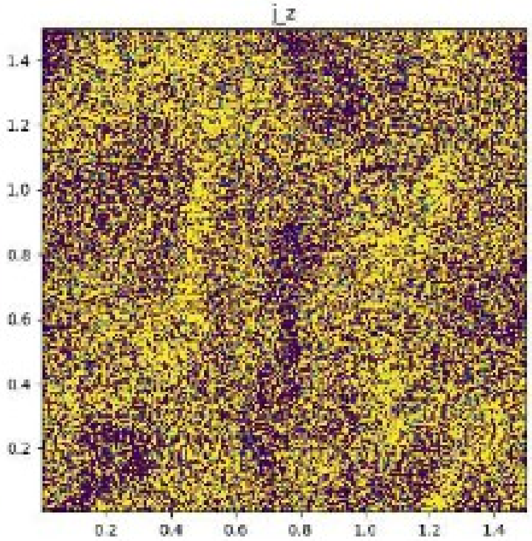

AGN application

$$B_r = 0, B_\theta = J_1(k_2 r), B_z = J_0(k_2 r),$$

Cylindrical coordinates, Bessel functions J0 and J1.

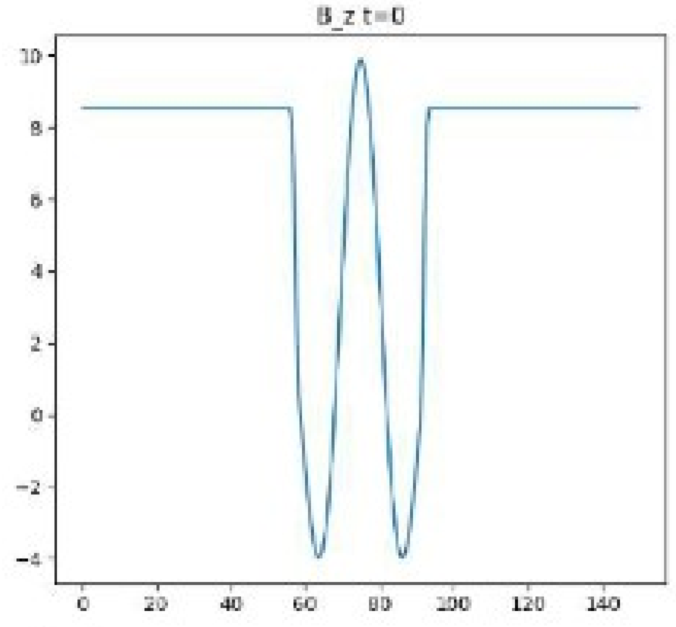

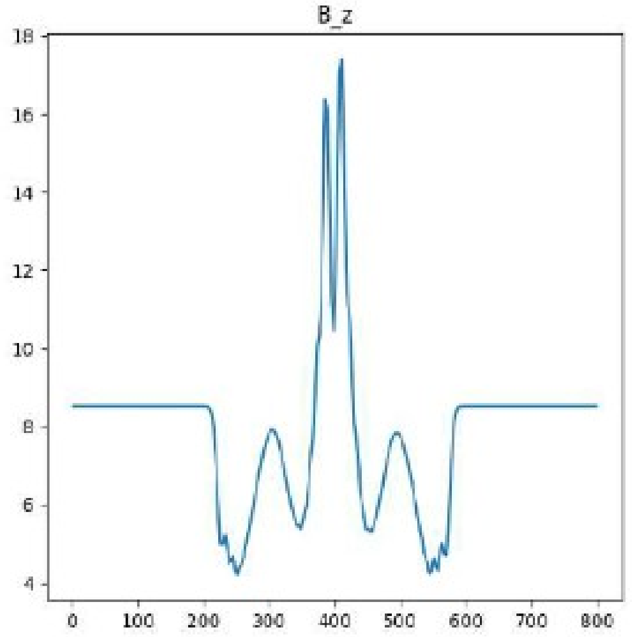

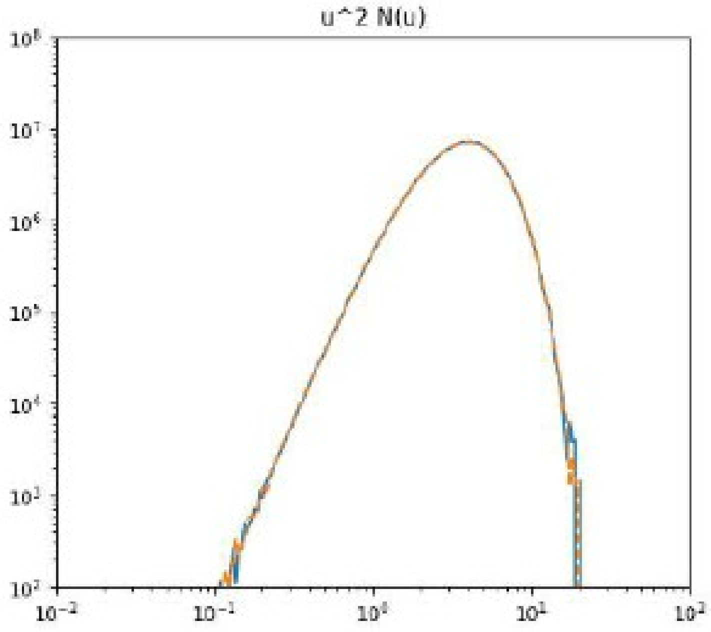

References

- Chen Q, Nalewajko K, Mishra B. Scaling of magnetic dissipation and particle acceleration in ABC fields. *Journal of Plasma Physics*. 2021;87(2):905870224. doi:10.1017/S0022377821000209

- Birdsall, C.K., & Langdon, A.B. (1991). Plasma Physics via Computer Simulation (1st ed.). CRC Press. https://doi.org/10.1201/9781315275048

- Cerutti B., Werner G.R., Uzdensky D.A., and Begelman M.C., The Astrophysical Journal 770, 147 (2013)